C_{60} Solvate with (1,1,2)-Trichloroethane: Dynamic Statistical Disorder and Mixed Conformation

Efstratia Mitsari,[1] *Michela Romanini,*[1] *Navid Qureshi,*[2] *Josep Lluís Tamarit,*[1] *Maria Barrio,*[1] *and Roberto Macovez* [1,*]

[1] Grup de Caracterització de Materials, Universitat Politècnica de Catalunya (UPC), ETSEIB, Departament de Física, Av. Diagonal 647, 08028 Barcelona, Spain

[2] Institut Laue-Langevin, 71 Av. des Martyrs - CS 20156 - 38042 GRENOBLE CEDEX 9, France

ABSTRACT

We present a full characterization of the orientationally disordered co-crystal of C_{60} with (1,1,2)-trichloroethane ($C_2H_3Cl_3$) by means of x-ray diffraction, Raman spectroscopy and broadband dielectric spectroscopy. Our results include the determination of molecular conformations, lattice structure, positional disorder, and molecular reorientational dynamics down to the microsecond timescale. We find that, while in the disordered solid phase of pure $C_2H_3Cl_3$ the molecules exist only in the *gauche* conformation, both *gauche* and *transoid* conformers are present in the solvate,

* Corresponding author. Tel: +34 934016568. E-mail: roberto.macovez@upc.edu.

where they occupy the largest interstitial cavities between the fullerenes species. The two $C_2H_3Cl_3$ conformers exhibit separate, independent relaxations, both characterized by simply-activated behavior. The relaxation of the *transoid* conformer, which has twice the dipole moment of the *gauche* isomer, is significantly slower than that of the latter, due to the high polarizability of C_{60} resulting in an electrostatic drag against the reorientations of the dipolar $C_2H_3Cl_3$ species. The observation of two distinct, simply-activated relaxations freezing at distinct temperatures indicates that they are not truly many-body relaxations, which may be rationalized considering that the $C_2H_3Cl_3$ molecules are separated by the relatively bulky C_{60} spacers.

Introduction

Molecular solids can display complete translational and rotational order (*molecular crystal*), sometimes with the existence of distinct crystallographic phases (polymorphism), or complete rototranslational disorder (*molecular glass*). In between these two extremes, molecular solids also display phases with only partial disorder: for example, phases in which all molecules have the same or similar orientation but no translational order (*liquid crystals*), or phases in which the molecules' average centers of mass occupy lattice positions while their orientations are disordered (*orientationally disordered solids*, a prominent example of which are plastic crystals). Last but not least, molecules possessing distinct isomers may be present in the same phase in different isomeric forms (*conformationally disordered solids*). Orientationally disordered (OD) phases exhibit many of the phenomenological features of glass formers, including a continuous slowing down of reorientational motions upon cooling which in some cases leads to the formation of an orientational glass in which all rotations are frozen.[1,2,3] Contrary to structural glasses, which do not exhibit any long-range order, OD solids are characterized by a translationally ordered structure and can therefore be more thoroughly characterized with the help of methods that exploit the translational symmetry such as Bragg diffraction, lattice models, or solid-state NMR spectroscopy.[4] OD phases are thus model systems for the experimental investigation of the glass transition, which is one of the unsolved fundamental problems of condensed matter science, and especially of the effect of translational invariance, anisotropy, and low-dimensionality on the glassy behavior.[5,6]

OD solids are generally formed by small molecules such as methane[7,8,9] or ethane derivatives,6,[10,11,12] or by globular molecules such as adamantanes[13,14] or fullerenes.[15,16] Research on OD phases has lead to important, in some instances unexpected, discoveries: for

example, studies on orientationally disordered fullerene (C_{60}) films have highlighted that orientational melting and solid-solid transitions are fundamentally modified at the surface of an OD phase.[17,18] Studies on solvents that display below their melting point either a supercooled liquid phase or an OD solid phase depending on the thermal treatment showed quite surprisingly that the glass transition is governed to a large extent by the freezing of the orientational degrees of freedom rather than translational ones.1',[19,20,21,22] A recent study has shown that solid OD phases can also display features typical of liquids such as viscous drag against molecular diffusion, leading to the validity of the Stokes-Einstein and Walden relations.3',[10] Also, it has been recently shown that the anisotropy of intermolecular interactions in OD solids can give rise to "bimodal" primary relaxations, with distinct cooperative molecular motions contributing to the primary dielectric loss.[23,24]

Fullerite (solid C_{60}) is a particularly simple and interesting example of OD phase. At room temperature, fullerite displays a so-called crystalline "rotator" phase in which the molecules spin as free rotors. Below 260 K the free-rotor motion is reduced to a merohedral ratcheting motion between two preferred orientations,[15,16] which freezes out at the glass transition temperature of 90 K.[25,26] OD phases with free-rotor or merohedral disorder have been identified also in many C_{60} intercalation compounds, such as inorganic co-crystals like alkali fullerides,[18,27] or molecular co-crystals of C_{60} with organic intercalants.[28,29,30, 31] Binary C_{60} co-crystals are simple systems to study the effects on rotational degrees of freedom of heteromolecular interactions (specifically, between C_{60} and the organic intercalants).[29,30,32,33,34,35] Solid-state NMR studies and molecular dynamics simulations on these systems showed that the C_{60} rotational motion is generally unhindered even when it is intercalated with guest molecules,[36,37] a prominent example being the "rotor-stator" C_{60} solvate with cubane.[29]

While several studies focused on the molecular dynamics of C_{60} inside binary co-crystals, very few studies focused on the dynamics of the intercalant molecules, most of which limited to establishing the existence of dynamic disorder of the intercalants.[30,36,38,39,40] Studies on the intercalant dynamics were performed on the C_{60} solvate with $Fe(C_5H_5)_2$,[37] and on the cubane solvate, where however the intercalant molecules have fixed orientations.[41] Probing the dynamics of both host and guest molecules can shed light on possible correlations between the dynamics of different species, and thus help understand from an experimental perspective the dynamic interactions (steric, van der Waals, dipolar, etc.) taking place between different molecules. Such knowledge may have a direct relevance for organic and biological systems, where the different chemical species present generally display correlated dynamics.[42,43,44]

In this contribution, we study the binary system consisting of the polar solvent (1,1,2)-trichloroethane ($C_2H_3Cl_3$) and the nonpolar Buckminster fullerene molecule (C_{60}). This binary system is particularly interesting because both C_{60} and $C_2H_3Cl_3$ display disordered solid phases,[15,16,25,26,45] and together they form a stable solvate (fullerene solvates are translationally ordered compounds obtained by evaporation of C_{60} solutions in suitable solvents).[32] We find that the C_{60}:$C_2H_3Cl_3$ solvate is a dynamically disordered crystal in which the ethane derivatives, which exist in two different conformations, are mainly surrounded by fullerene first neighbors. This results in two distinct reorientational relaxation processes (one for each conformer), both of which exhibit pronounced non-cooperative character due to the limited interactions between $C_2H_3Cl_3$ molecules and the large polarizability of the C_{60} spacers.[46,47,48]

Experimental Methods

Sample preparation

Buckminsterfullerene C_{60} and (1,1,2)-trichloroethane ($C_2H_3Cl_3$) were purchased from Aldrich with purities 99.5 % and 99 %, respectively. The $C_2H_3Cl_3$ solvent was distilled twice at 385 K before use. The formation of the C_{60}:$C_2H_3Cl_3$ solvate was already reported in Ref. 32, in a study which also specified the symmetry of the solvate structure and the stability inside the mother liquor for prolonged periods of time. Briefly, dissolutions of C_{60} in $C_2H_3Cl_3$ were allowed to evaporate in the dark at room temperature, yielding a powder composed of plate-like and needle-shaped crystals. The sample was probed by thermogravimetry, calorimetry, powder and single-crystal X-ray diffraction, Raman spectroscopy and broadband dielectric spectroscopy. Grinding and application of hydraulic pressure to the samples were avoided due to the tendency of the solvate to decompose under mechanical treatment,[32] as observed also in other C_{60} solvates.[49]

Thermogravimetry characterization of the solvate powder (not shown) shows a mass loss of about 15% upon desolvation, which is consistent with the 1:1 stoichiometry of the solvate. The phase behavior of the synthesized powder, as measured by calorimetry, was similar to that reported in Ref. 32. Thermal analyses carried out on the solvate polycrystalline powder indicate a desolvation temperature of 420 K, slightly lower than that of the solvate single crystal (440 K).[32]

Sample characterization

High-resolution X-ray powder diffraction (XRPD) profiles were recorded with a vertically mounted INEL position-sensitive cylindrical detector (CPS120). Monochromatic Cu Kα1 radiation was filtered with an asymmetric-focus curved quartz monochromator. The solvate powder was placed in a Lindemann capillary tube (0.5 mm diameter). The detector was used in the Debye-Scherrer geometry (transmission mode), yielding diffraction profiles over a 2θ range between 4° and 40° with an angular step of 0.029° (2θ). Analysis of the diffraction data was carried out using the Fullprof software by comparing the experimental data, including the single

crystal data published in Ref. 32, with different microscopic models for the molecular arrangements. The FullProf package offers the possibility to refine a single structure model on multiple data sets (such as a powder and a single-crystal data set) with relative weights. Instead, a structure analysis based exclusively on the single-crystal data (which included only 29 reflections) was not possible due to the large number of refinement parameters.

For dielectric measurements, the solvate powder was mechanically pressed between two stainless steel disks to obtain a pellet inside the parallel plate capacitor formed by the metal disks. The dielectric spectra were acquired in the frequency range from 10^{-2} to 10^{6} Hz with a Novocontrol Alpha analyzer. Temperature control was achieved by nitrogen-gas flow, which allowed measuring in a temperature interval between 120 and 300 K with a temperature stability of 0.2 K.

Raman Microscopy was employed to record spectra at room temperature in the wavenumber range between 50 cm^{-1} and 2500 cm^{-1} (at higher wavenumbers a fluorescence signal dominated the spectra). For this purpose, a LabRam HR 800 system with excitation laser wavelength of 532 nm (green) was used. The Raman scattering spectra were measured with ten accumulations (with acquisition time of 30 s) and low laser power (0.05 mW) so as to avoid any photodecomposition. Pure C_{60} powder and liquid (1,1,2)-trichloroethane were also characterized for comparison. For the liquid only 5 accumulations were used each with acquisition time of 5 s, and the laser power was set to 5 mW.

Results and Discussion

XRD Patterns and Structural Modeling

When co-crystallized with solvent or guest molecules, C_{60} forms a large variety of structures depending on the size of the solvent/guest molecules compared with that of the C_{60} species.[28] In

the case of the C_{60}:$C_2H_3Cl_3$ solvate, a single-crystal study[32] reported orthorhombic lattice metrics but with monoclinic symmetry of space group $P2_1/n$. The monoclinic symmetry departs from the orthorhombic symmetry of similar C_{60} solvates with 1:1 stoichiometric ratios, such as the ones with *n*-pentane, *n*-hexane or dichloroethane.[34,35,50] The room-temperature powder XRD pattern of C_{60}:$C_2H_3Cl_3$ (Figure 1) is consistent with the monoclinic symmetry. A symmetry lower than orthorhombic could be due to an anisotropic orientational disorder of the ethane derivatives or result from the fact that the $C_2H_3Cl_3$ molecules do not possess a mirror plane symmetry. To explore this issue, we modeled both powder and single-crystal diffraction patterns using different assumptions on the conformation, position and orientation of each molecular species.

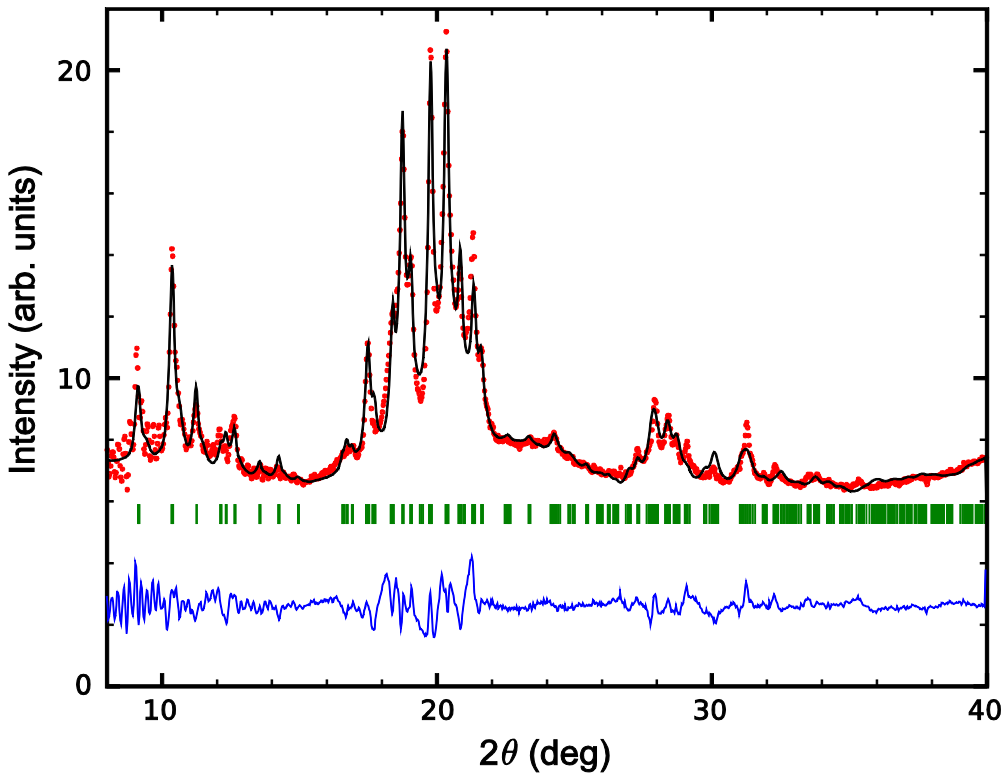

Figure 1. Experimental X-ray powder diffraction patter of the C_{60}:$C_2H_3Cl_3$ solvate (red markers), together with its fit (superposed solid line) and the respective difference (lower solid line). Vertical bars indicate the refined angular Bragg peaks.

The powder diffraction pattern and the single-crystal intensities were analyzed using a rigid-body model for both the C_{60} and the $C_2H_3Cl_3$ molecules. The data was also analyzed using symmetry-adapted spherical harmonics in order to mimic a possible orientational disorder of the C_{60} molecules, yielding similar results. This suggests that the C_{60} molecules might display dynamic orientational disorder, as found in several solvates.[29,30,51] Refined parameters of the crystal structure were the lattice constants, the positions of the molecules, their orientation, the isotropic temperature factors and the occupation factors. The quite broad diffraction profiles could only be described by introducing positional and orientational disorder of the C_{60} moieties. The C_{60} positional disorder was simulated by considering two nonequivalent molecular positions in the unit cell, *p1* and *p2*, and fixing the sum of the respective occupation factors to unity.

The refinement of the powder data clearly reveals the positions of the C_{60} molecules and provides the lattice symmetry and parameters. The average lattice parameters deduced from the powder data are a = 10.1302(5) Å, b = 31.449(2) Å, c = 10.1749(5) Å, with a monoclinic angle β = 90.14(8)°. The matrix formed by the fullerene units can be described as the stacking, along the b crystallographic axis of C_{60} layers parallel to the *ac* plane with a square-like base of side equal to the closest inter-fullerene separation (~10 Å). This is visible in Figure 2, where the refined structure of the C_{60}:$C_2H_3Cl_3$ solvate is depicted. The stacking order of the square-like planes is of the type AB-B'A'-AB. In units of the unit cell parameters, B is shifted by (x+½, –y+½, z+½) with respect to A, and B' and A' are shifted by (–x+½, y+½, –z+½) with respect to A and B, respectively, where the fractional coordinates x, y and z refer to the position (*p1* or *p2*) of a C_{60}

molecule within the A layer. The positions *p1* and *p2* of the centers of mass of the two nonequivalent fullerene molecules in the A layer are listed in Table 1. The positional disorder is mainly along the *b* axis, and leads to a significant overlap of *p1* and *p2* molecules in the unit cell. The positional disorder corresponds to a locally-varying separation (orthogonal distance) between the AB and B'A' bilayers. It is worth pointing out that two nonequivalent C_{60} positions were also reported in the fullerene solvate with benzene (C_{60}:4C_6H_6).[52] We argue that the existence of different C_{60} sites is related to a static structural disorder associated with the relatively poor crystallinity of the powder, rather than to a dynamic translational disorder.

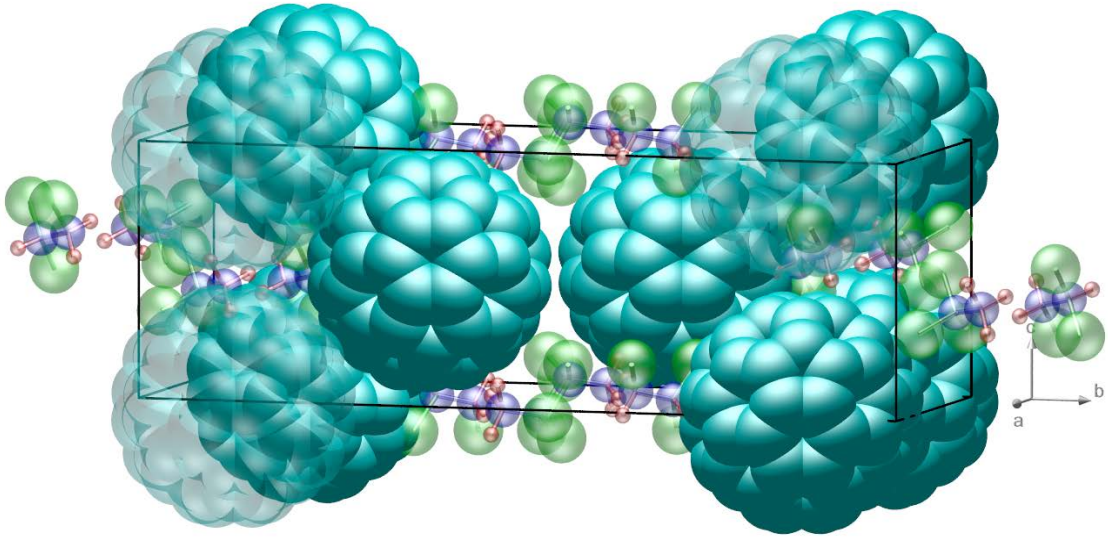

Figure 2. Visualization of the refined crystal structure of the C_{60}:$C_2H_3Cl_3$ solvate. The cuboid represents the monoclinic unit cell. For clarity, only the averaged centers of mass of the C_{60} molecules are shown, and some fullerenes are displayed with a transparency to better visualize the positions of the other molecules. Both *transoid* and *gauche* $C_2H_3Cl_3$ conformers are present, and for each conformer both refined positions are shown, to emphasize the filling of the interstitial cavities between the C_{60} molecules (two $C_2H_3Cl_3$ molecules occupy each cavity).

The excess electron density between the C_{60} species is attributed to the contribution of orientationally disordered $C_2H_3Cl_3$ molecules. The $C_2H_3Cl_3$ positions were refined by reproducing the extra diffraction intensity not accounted for by the contribution of the C_{60} species. As visible in Fig. 2, relatively large interstitial cavities separate fullerene molecules along the direction parallel to the *b* axis. These interstitial sites are large enough to accommodate at least two ethane derivatives (instead, the $C_2H_3Cl_3$ molecules are too big to fit in the octahedral cavities of pristine fullerite), and due to the symmetry of the crystallographic space group and the obtained positions of the $C_2H_3Cl_3$ molecule, there are always two molecules within a cavity, connected by an inversion center.

Two distinct positions and orientations of either two *transoid*, two *gauche* or one of each conformer were refined, restricting the total occupation to one molecule per formula unit. From the powder data alone it was not possible to deduce the distribution of the different conformers, because also populations of 100% *transoid* or 100% *gauche* conformers yielded comparable results (R_F = 4.02). However, a correlated refinement between the powder and the single crystal data strongly favors the scenario with two conformers (the agreement factors of the correlated refinement are $R_{F,p}$ = 8.95 and $R_{F,sc}$ = 22.1, while the refinements using exclusively *transoid* or *gauche* diverged). The existence of both conformers is confirmed by the characterization by dielectric spectroscopy and Raman (see the next subsection).

The obtained positions of both the *transoid* and *gauche* conformers are listed in Table 1. As visible in Figure 2, the stacking of fullerene planes along the *b* direction is interrupted by interstitial $C_2H_3Cl_3$ molecules arranged in pairs; the translational disorder of the C_{60} molecules along the b axis is therefore related to the disordered arrangement of the (1,1,2)-trichloroethane molecules in the interstitial cavities. Inspection of the refined atomic positions indicates that the

ethane derivatives display a tendency to orient themselves with a C–halogen bond rotated towards the closest C_{60} neighbor, as reported for example also in the case of the C_{60} solvates with bromobenzene (C_{60}:$2C_6H_5Br$) and with benzene and diiodomethane (C_{60}:CH_2I_2:C_6H_6).[53,54] Both the C_{60} and the $C_2H_3Cl_3$ molecules occupy a single general 4e Wyckoff site, which in particular means that all the $C_2H_3Cl_3$ molecules of the same conformation have the same crystallographic environment. The detailed structural data are available as CIF file as Supporting Information.

Table 1. Molecular center-of-mass positions obtained by correlated refinement between powder and single-crystal diffraction data.*

	C_{60} *p1*	C_{60} *p2*	$C_2H_3Cl_3$ *transoid*	$C_2H_3Cl_3$ *gauche*
x	0.218(4)	0.193(2)	0.90(3)	0.76(1)
y	0.169(2)	0.122(2)	0.67(1)	0.571(4)
z	0.004(3)	-0.003(2)	0.06(6)	0.09(1)
occupancy	0.46(2)	0.54(2)	0.25(1)	0.75(1)

*The positions of each molecule (two of each kind) are given in units of the lattice constants deduced from the powder data.

Dielectric Relaxations and Raman Spectroscopy Results

The dielectric spectra of the solvate are shown in Figure 3. It is clear from visual inspection of e.g. the spectra at 180 and 195 K that two distinct relaxation features are present, with comparable dielectric strength (see inset to Figures 3 and Figure 4(b)). Both dielectric features are due to dipolar moieties present in the solvate. Since $C_2H_3Cl_3$ is polar while C_{60} is apolar, we ascribe both relaxations in the solvate to the dynamics of (1,1,2)-trichloroethane molecules. The observation of dynamic processes indicates that the disorder highlighted by the analysis of XRD data is actually dynamic in character, at least for what concerns the ethane derivatives.

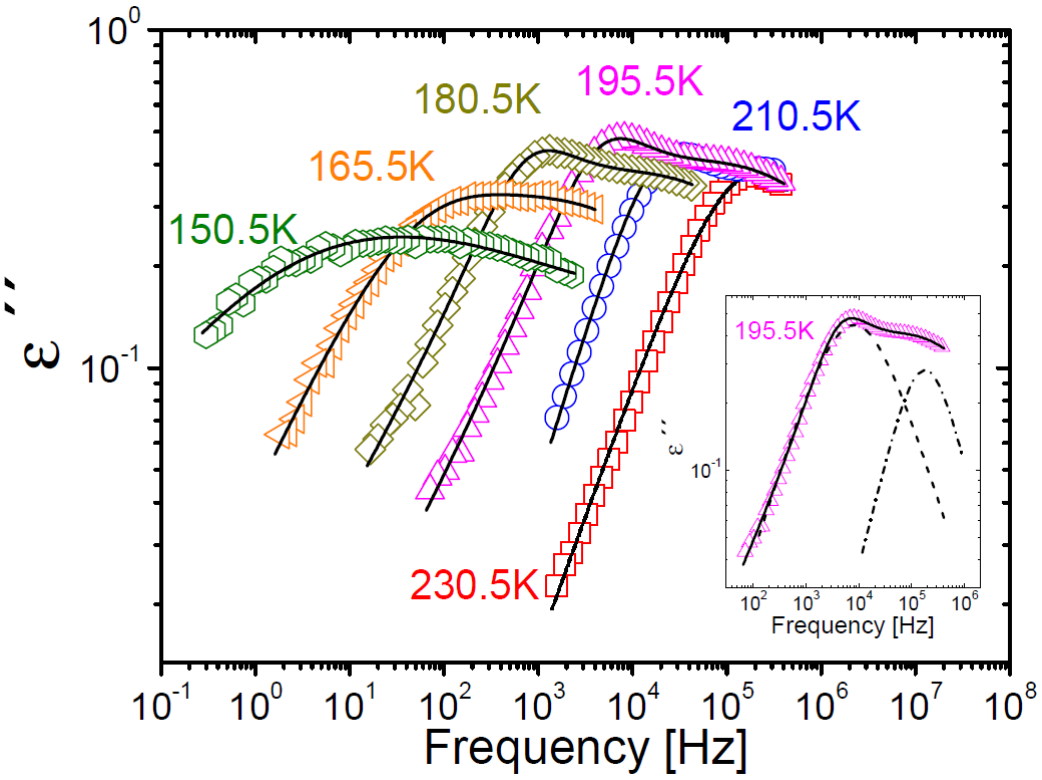

Figure 3. Dielectric loss spectra of the C_{60}:$C_2H_2Cl_3$ solvate, at selected temperatures. Continuous lines are fits assuming a Cole-Cole profile of each loss feature (see the text). Inset: visualization of both components (dashed and dash-dotted lines) in the fit of the spectrum acquired at 195.5 K.

In order to carry out a quantitative analysis, both dielectric loss features were fitted by a Cole-Cole function, whose analytic expression is:[55,56]

(Eq. 1) $\varepsilon_{CC}(f) = \varepsilon_\infty + \frac{\Delta\varepsilon}{1+(i2\pi f\tau)^\beta}$.

Here $\Delta\varepsilon = \varepsilon_s - \varepsilon_\infty$ is the dielectric strength, ε_∞ and ε_s are the high-frequency and static low-frequency limits of the real permittivity, β is a (temperature-dependent) shape parameter in the range from 0 to 1, and τ represents the characteristic time of molecular motions, defined as the time at which the dielectric loss is maximum and referred to as relaxation time. Figure 4(a) shows the relaxation time τ for both $C_2H_3Cl_3$ relaxations as a function of the inverse temperature

(Arrhenius plot). The dielectric strength of each process, depicted in Figure 4(b), is found to be basically independent of temperature, while the exponent β of the Cole-Cole distribution (Figure 4(c)) is found to decrease with decreasing temperature. A lower Cole-Cole exponent implies a wider distribution of relaxation times, consistent with the increased spectral width at low temperature (compare for example the loss spectra at 195.5 and 150.5 K in Fig. 4). Such increase in spectral width with decreasing temperature is common to many systems.[57]

It is observed in figure 4(a) that both relaxations exhibit, at least approximately, a simply-activated (Arrhenius) temperature dependence, *i.e.*, a functional dependence of $\tau(T)$ of the form:

(Eq. 2) $\tau(T) = \tau_\infty \exp\left(-\frac{E_a}{k_B T}\right)$.

Here, E_a is the activation energy and τ_∞ is the so-called attempt time, corresponding to the value of the relaxation time in the high-temperature limit ($T \to \infty$, *i.e.* $1/T \to 0$). The activation energies of both solvate relaxations (see Figure 4(a)) are virtually identical, namely 0.37±0.02 eV for the slower (lower-frequency) relaxation and 0.36±0.03 eV for the faster (higher-frequency) one, or equivalently, approximately 36 kJ/mol in both cases. By extrapolating the Arrhenius behavior to high temperature, the attempt time of the two relaxations are obtained as $\mathrm{Log}(\tau_\infty) = -14$ and $\mathrm{Log}(\tau_\infty) = -15$ for the slower and faster relaxations, respectively. These values are in agreement with the expectation for a non-cooperative process at high temperature, and are typical values found for dielectric relaxations in glass-forming systems. We point out that, since at low temperature we cannot reliably separate both contributions to the dielectric loss due to the increased spectral width, we cannot exclude a deviation from the simply-activated behavior (Eq. 2) at low *T*.

It is worth pointing out that both the simply-activated nature and the Cole-Cole profile of the relaxation features are uncommon for α relaxations associated with a glass transition,[1] and are

instead typical of primary relaxations in non-viscous, non-polar solvents or of so-called secondary (local) relaxations in glass formers.[57] In the solvate, the $C_2H_3Cl_3$ molecules are expected to interact only weakly with one another. Each $C_2H_3Cl_3$ has only one $C_2H_3Cl_3$ first neighbor, namely the molecule that shares the same cavity, while all other next-neighbors are fullerenes (Fig. 2). Apart from the solvent molecules sitting in the same interstitial site, the separation between ethane derivatives is thus larger than the van der Waals diameter of the C_{60} molecule, which is of the order of 1 nm,[58] leading to a relatively large inter-molecular separation compared with pure $C_2H_3Cl_3$. In other words, the polarization interactions with the quasi-spherical fullerene molecules are particularly strong, while interactions between $C_2H_3Cl_3$ molecules (dipole-dipole or steric) are less important. This discussion indicates that the observed relaxation dynamics are at most only weakly cooperative, and can be classified as (local) secondary relaxations.

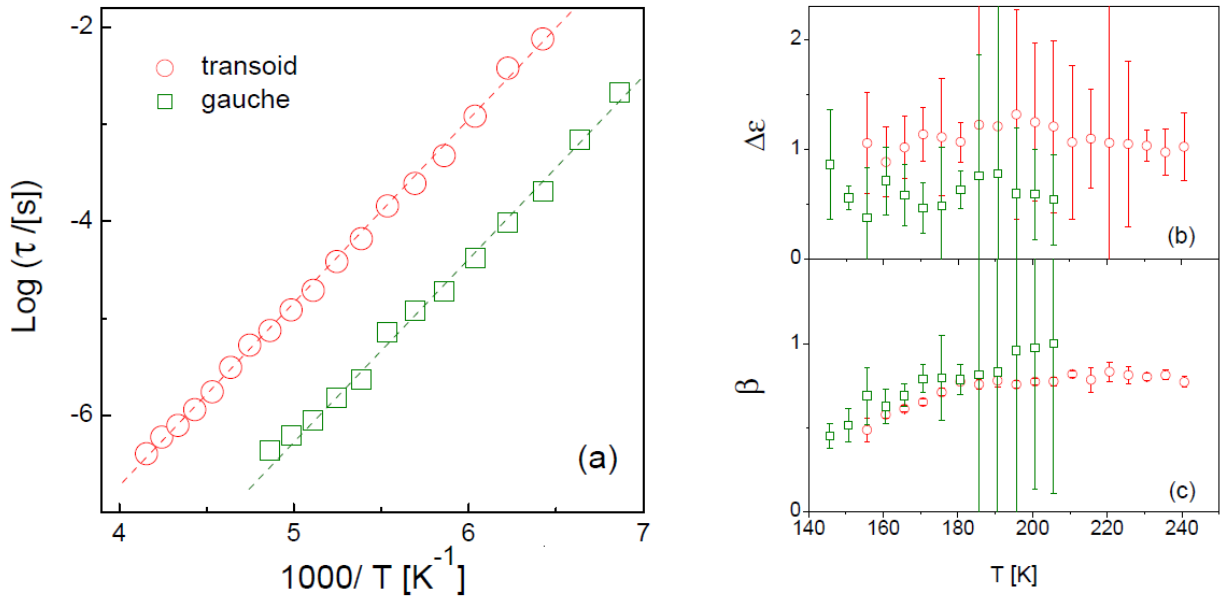

Figure 4. (a) Arrhenius plot of the relaxation times τ of $C_2H_3Cl_3$ molecules in the solvate (markers), together with their Arrhenius fits with Eq. 2 (dashed lines). (b, c) Dielectric strength $\Delta\varepsilon$ (b) and Cole-Cole exponent β (c) of both solvate relaxations, as a function of temperature (see Eq. 1). In all panels, open circles (respectively, squares) represent the transoid (resp., gauche) relaxation.

Given that all the crystallographic sites occupied by the solvent molecules are very similar, the observed difference in relaxation time between both dynamic processes cannot be due to the different positions occupied by the $C_2H_3Cl_3$ molecules. Instead, it is likely that the origin of the two relaxations is the isomerism of the ethane derivatives. The two $C_2H_3Cl_3$ conformers have quite different dipole moments, of magnitude 1.44 D for the *gauche* isomer and 2.95 D (*i.e.*, more than twice as much) for the *transoid* isomer. [59,60] We thus assign each relaxation process to the reorientational dynamics of a different (1,1,2)-trichloroethane conformer. On the other hand, *transoid-gauche* and/or *gauche–gauche* isomer fluctuations would not result in two relaxations well separated in frequency. Moreover, conformational relaxations are expected to be significantly faster than the observed dynamics. A preliminary study on the conformationally-disordered solid phase of (1,1,2)-trichloroethane, where isomeric fluctuations take place, indicates that the corresponding dynamics is indeed significantly faster than either dynamic process in the solvate, confirming our interpretation of the dielectric loss features as being associated with a dynamic *orientational* disorder.

To confirm the presence of both conformers, we carried out a Raman spectroscopy characterization. Vibrational and NMR studies on the pure solvent have shown that the $C_2H_3Cl_3$ molecules exist in both conformations[59] in the liquid phase, with comparable concentrations,[61,62,63,64] and that each conformer has a specific vibrational signature.[60,65] Given

that two conformers are present in the solution used to form the solvate, it is possible that they are also present in the solvate; however, the occurrence and relative concentration of conformers varies according to the nature of the system,[66] and depends on the subtle balance of intramolecular strains and the effects of the molecular environment.[45] For example, the *gauche* conformer is energetically more stable and by far the most abundant in the gas phase,[65,60] where intermolecular interactions are negligible. In the disordered solid phase of pure $C_2H_3Cl_3$ only *gauche* conformers are present, and they undergo dynamic conformational changes between isomers of different chirality.[45] Quite oppositely, in the fully ordered crystalline solid phase of (1,1,2)-trichloroethane only *transoid* conformers are observed.

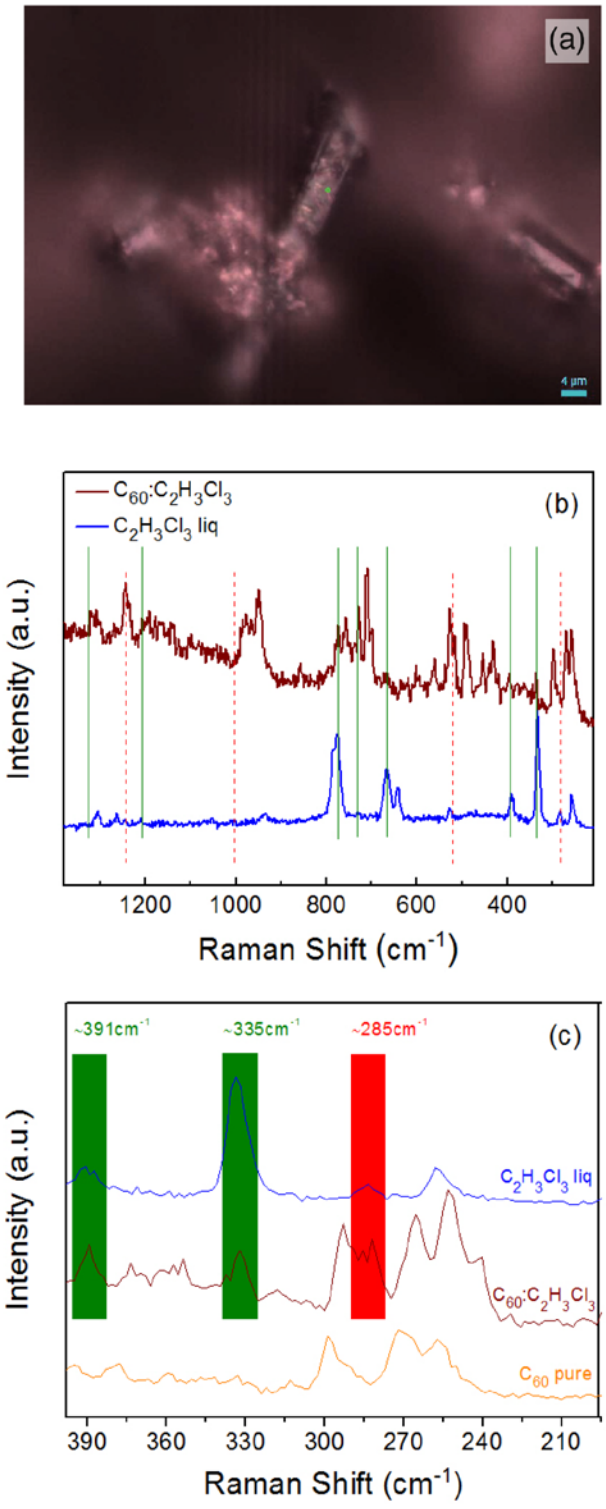

Figure 5. (a) Raman microscopy image of solvate crystallites. The bright green spot is produced by the excitation laser and indicates the position where the Raman spectrum of the solvate in (c)

was acquired. (b) Raman spectra of the C_{60}:$C_2H_3Cl_3$ solvate (wine, upper curve) and of liquid $C_2H_3Cl_3$ (blue, lower curve) between 200 and 1400 cm^{-1}. The vibration wavenumbers of modes corresponding exclusively to either the *transoid* or *gauche* $C_2H_3Cl_3$ conformers are highlighted with vertical (red) dashed lines and (green) solid lines, respectively. (c) Raman spectra of liquid $C_2H_3Cl_3$ (blue upper curve), of the C_{60}:$C_2H_3Cl_3$ solvate (wine, middle curve) and of pure solid C_{60} (orange, lower curve), in the region between 200 and 400 cm^{-1}. The peaks in the spectral regions highlighted in green are due to skeletal deformations of the *gauche* conformer, while that in the red shaded region is due to skeletal vibrations of the *transoid* conformer.

We acquired Raman spectra both on the polycrystalline C_{60}:$C_2H_3Cl_3$ powder, on pristine C_{60} and on the pure liquid solvent (always using the same substrate), to positively identify the weak features corresponding to different conformers. Figure 5(a) shows a Raman micrograph of solvate crystallites, where a rectangular platelet and a ten-sided prism can be observed. The crystallite shapes are similar to those observed in the SEM photographs of the solvate in Ref. 32.

Figure 5(b) shows the Raman spectrum of the C_{60}:$C_2H_3Cl_3$ solvate, compared to that of the pure $C_2H_3Cl_3$ solvent. The solvate spectrum includes vibrations of both solvent and C_{60} molecules, the contribution of (1,1,2)-tricloroethane being relatively small due to the relatively small volume density of these molecules in the solvate. The relatively poor signal-to-noise ratio in the solvate spectrum might also be due to possible inhomogeneities in the material. Based on the Raman results presented in Ref. 59, we are able to assign some of the vibrational modes of the C_{60}:$C_2H_3Cl_3$ solvate to either *gauche* or *transoid* $C_2H_3Cl_3$ conformers, and thereby conclude that both conformers are present in the solvate. In particular, the vibrations at wavenumbers of 335, 391, 666, 730, 774, 1211 and 1325 cm^{-1} (solid vertical lines in Fig. 5(b)) correspond to the *gauche* isomer, and those visible at 285, 525, 1008 and 1241 cm^{-1} (dashed lines) stem from the

transoid isomer. While the position of these bands did not change significantly with respect to liquid $C_2H_3Cl_3$, their intensities in the solvate were in general different from those of the pure solvent. The fact that the *gauche* Raman bands are more numerous and more intense on average suggests that the majority of ethane derivatives are in the *gauche* conformation.

Figure 5(c) shows a different Raman spectrum of the solvate platelet of Fig. 5(a) in the range between 200 and 400 cm^{-1} (middle curve), together with that of the liquid solvent (upper curve) and that of pristine fullerite (lower curve) for comparison purposes. In panel (c) the *gauche* isomer bands at 335 and 391 cm^{-1} are clearly visible, as is the *transoid* peak at 285 cm^{-1}. While all three bands are also visible in liquid $C_2H_3Cl_3$, they are absent in the Raman spectrum of pristine fullerite. These results show that both conformations of (1,1,2)-trichloroethane are present in the solvate.

In organic binary systems containing $C_2H_3Cl_3$, between the two conformers the intermolecular interactions of $C_2H_3Cl_3$ with the other organic co-solvent shifts the conformational equilibrium due to the large difference in dipole moment of the two conformers; their relative abundances depend on the dielectric constant of the mixture and the molecular structure of co-solvent.[60] In the solvate with C_{60}, dipolar interactions between the ethane derivatives are weaker than in the solid phases of $C_2H_3Cl_3$ due to the presence of the C_{60} spacers.[67,68] Moreover, due to the disorder present in this phase they might be more isotropic compared to solid $C_2H_3Cl_3$ phases and similar in strength to those of the pure liquid solvent, which might rationalize the occurrence of both isomers in the solvate.

As mentioned, both solvate relaxations exhibit very close activation energies (36 kJ/mol in both cases), which might be due to the fact that the molecular environment of both conformers is the same. On the other hand, the two dynamic processes are observed at quite different relaxation

times; such difference is likely due to the fact that the motion of the $C_2H_3Cl_3$ dipoles in the solvate is hindered by the high polarizability of the C_{60} matrix,[46,47,48,69] resulting in a polarization cloud which must rearrange at each reorientation of the $C_2H_3Cl_3$ molecule and therefore to an effective electrostatic drag acting against the orientational dynamics. Since the induced polarization is larger in the case of the larger permanent dipole of the *transoid* conformer, we assign the slower reorientational motion at lower frequency (longer characteristic times) to the *transoid* isomer, and the faster one to the *gauche* isomer. The freezing temperature of the two motions, defined as it is customary as the temperature at which a given process reaches a characteristic relaxation time of 100 seconds,[70] can be extrapolated assuming that their simply-activated behavior holds for all temperatures; the freezing temperature of the *transoid* relaxation is found to be approximately 170 K while that of the *gauche* relaxation is around 100 K. If the relaxation of the (1,1,2)-trichloroethane molecules were a cooperative process, one would expect a single (glass-transition) temperature to mark the simultaneous freezing of the cooperative dynamics. The observation of two non-converging relaxations corroborates therefore the non-cooperative, single-molecule-like nature of the molecular dynamics in the solvate, and rationalizes the observation of separate dynamics for each conformer (*i.e.*, for distinct magnitude of the molecular dipole).

With this assignment, it is found that the dielectric strength ($\Delta\varepsilon$) of the *transoid* relaxation ($\Delta\varepsilon_{transoid}$ = 1.1±0.1) is roughly twice that of the *gauche* relaxation ($\Delta\varepsilon_{gauche}$ = 0.6±0.2), as depicted in the inset to Fig. 4. The dielectric strength of a relaxation involving a dipolar moiety is proportional to the square of the molecular dipole moment μ and to the density of dipoles (N),[70] *i.e.*, $\Delta\varepsilon \propto \mu^2 N$. The proportionality coefficient actually contains the so-called Kirkwood correlation factor,[71] which describes the degree of correlation between the relative orientations of

(nearest-neighbor) dipoles during the reorientation dynamics.[70,72] In view of the similar origin of the two relaxation processes, one may assume that the Kirkwood correlation factor is approximately the same for both dynamics. Under this assumption, and considering that the dipole moment of the *transoid* conformer is twice that of the *gauche* one, if the two conformers had equal populations their strength would differ by a factor of four. The fact that the two strengths are in a ratio close to 2 to 1 would instead indicate that the *gauche* conformation is more abundant in the solvate, in agreement with our Raman and XRD results.

As a final remark, we note that the observation in the solvate of molecular dynamics involving the ethane derivatives suggests that also the fullerene species may display merohedral reorientational motions in this phase. This would not be surprising considering that the C_{60} molecules usually display rotational dynamics also when intercalated with other organic molecules.[29,36,37]

Conclusions

We presented a full microscopic characterization of the dynamic statistical disorder in the solvate of C_{60} with (1,1,2)-trichloroethane ($C_2H_3Cl_3$). Our study included the determination in this solid phase of molecular conformations, lattice structure, positional and orientational disorder, and molecular dynamics down to the microsecond timescale. Both *gauche* and *transoid* conformations of the $C_2H_3Cl_3$ species are present in the solvate, with a majority of *gauche* conformers. The two conformers exhibit separate dynamics with simply-activated temperature dependence, implying that they are local, at most weakly cooperative, relaxations of $C_2H_3Cl_3$ molecules "diluted" in the fullerene matrix. The isomer with larger dipole moment conformer (*transoid*) polarizes more strongly the C_{60} moieties, resulting in a more pronounced electrostatic drag against dipole reorientations and thus slower reorientational motion compared to the *gauche*

conformer. The low degree of dynamic cooperativity in the solvate is evidenced by the fact that the two relaxations freeze at distinct temperatures. The lack of cooperativity, which contrasts with the collective character of molecular relaxation dynamics in most glass-forming systems, is due to the presence of the C_{60} molecules acting as highly polarizable spacers that effectively decouple the molecular dynamics.

Our study provides hard-to-obtain information on the molecular arrangement in a binary organic co-crystal, and to the best of our knowledge it is the first-ever report of the relaxation dynamics of guest molecules in C_{60} solvates. The obtained results show that the characteristic reorientational relaxation times of dipolar species depend on the details of intermolecular coupling such as dipole-induced dipole (polarization) interactions. Considering the very broad variety of structures with dynamic disorder that can be obtained with fullerene solvates with different solvent or guest molecules, orientationally disordered C_{60} solvates represent model systems to investigate the impact of the structure and thus of the interaction geometry on the molecular dynamics of heterogeneous polar systems.

ASSOCIATED CONTENT

Supporting Information. Crystallographic structure data for the C_{60}:$C_2H_3Cl_3$ solvate in crystallographic information file (CIF) format. This material is available free of charge via the Internet at http://pubs.acs.org.

AUTHOR INFORMATION

Corresponding Author

*Phone: 34-934016568. E-mail: roberto.macovez@upc.edu.

Author Contributions

The manuscript was written through contributions of all authors. All authors have given approval to the final version of the manuscript.

Notes

The authors declare no competing financial interests.

ACKNOWLEDGMENT

This work has been partially supported by the Spanish Ministry of Science and Innovation MINECO through project FIS2014-54734-P and by the Generalitat de Catalunya under project 2014 SGR-581.

Table of Contents Graphic

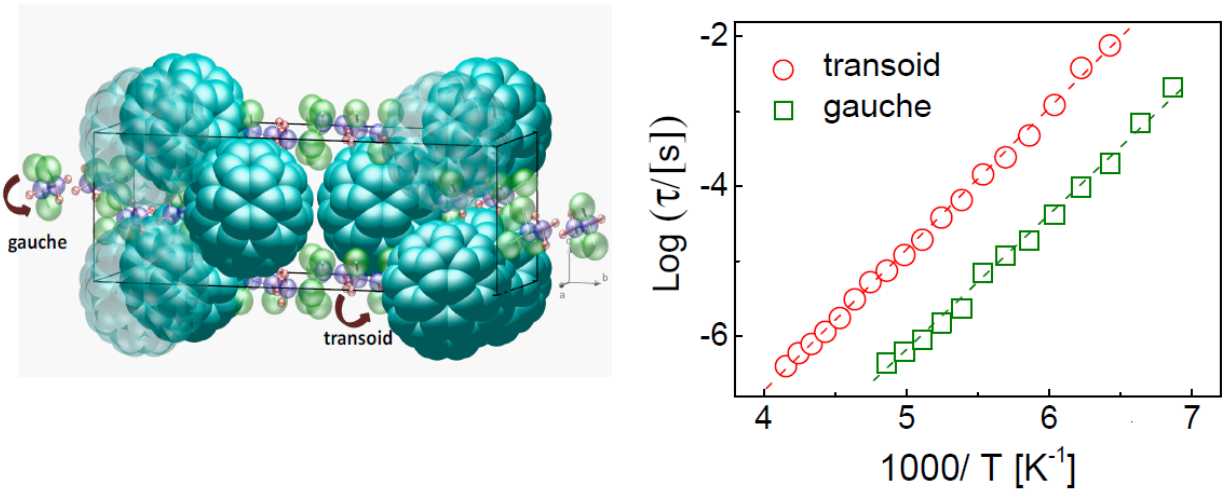

REFERENCES

[1] Brand R.; Lunkenheimer, P.; Loidl, A. Relaxation Dynamics in Plastic Crystals. *J. Chem. Phys.* **2002**, *116*, 10386-10401.

[2] Romanini, M.; Martinez-Garcia, J.C.; Tamarit, J. Ll.; Rzoska, S.J.; Barrio, M.; Pardo, L.C.; Drozd-Rzoska, A. Scaling the Dynamics of Orientationally Disordered Mixed Crystals. *J. Chem. Phys.* **2009**, *131*, 184504.

[3] Zachariah, M.; Romanini, M.; Tripathi, P.; Barrio, M.; Tamarit, J.Ll.; Macovez, R. Self-Diffusion, Phase Behavior, and Li+ Ion Conduction in Succinonitrile-Based Plastic Co-Crystals. *J. Phys. Chem. C* **2015**, *119*, 27298–27306.

[4] Pérez, S.C. ; Zuriaga, M. ; Serra, P. ; Wolfenson, A. ; Negrier, Ph.; Tamarit, J.Ll. Dynamic Characterization of Crystalline and Glass Phases of Deuterated 1,1,2,2 Tetrachloroethane. *J. Chem. Phys.* **2015**, *143*, 134502.

[5] Drozd-Rzoska, A.; Rzoska, S.J.; Pawlus, S.; Tamarit, J.Ll. Dynamics Crossover and Dynamic Scaling Description in Vitrification of Orientationally Disordered Crystal. *Phys. Rev. B* **2006**, *73*, 224205.

[6] Sharapova, I.V.; Krivchikov, A.I.; Korolyuk, O.A.; Jezowski, A.; Rovira-Esteva, M.; Tamarit, J.Ll.; Pardo, L.C.; Ruiz-Martin, M.D.; Bermejo, F.J. Disorder Effects on Heat Transport Properties of Orientationally Disordered Crystals. *Phys. Rev. B* **2010**, *81*, 094205.

[7] Zuriaga, M.; Pardo, L.C.; Lunkenheimer, P.; Tamarit, J.Ll.; Veglio, N.; Barrio, M.; Bermejo, F.J.; Loidl, A. A New Microscopic Mechanism for Secondary Relaxation in Glasses. *Phys. Rev. Lett.* **2009**, *103*, 075701.

[8] Krivchikov, A. I.; Vdovichenko, G. A.; Korolyuk, O. A.; Bermejo, F.J.; Pardo, L.C.; Tamarit, J.Ll.; Jezowski, A.; Szewczyk, D. Effects of Site-Occupation Disorder on the Low-Temperature Thermal Conductivity of Molecular Crystals. *J. Non-Cryst. Solids* **2015**, *407*, 141-148.

[9] Zuriaga, M. J.; Perez, S. C.; Pardo, L.C.; Tamarit, J.Ll. Dynamic Heterogeneity in the Glass-like Monoclinic Phases of $CCl_{4-n}Br_n$, n=0,1,2. *J. Chem. Phys.* **2012**, *137*, 054506.

[10] Zachariah, M.; Romanini, M.; Tripathi, P.; Tamarit, J.Ll.; Macovez, R. Molecular Diffusion and Dc Conductivity Perfectly Correlated with Molecular Rotational Dynamics in a Plastic Crystalline Electrolyte. *Phys. Chem. Chem. Phys.* **2015**, *17*, 16053–16057.

[11] Vdovichenko, G. A.; Krivchikov, A.I.; Korolyuk, O.A.; Tamarit, J.Ll.; Pardo, L.C.; Rovira-Esteva, M.; Bermejo, F.J.; Hassaine, M.; Ramos, M.A. Thermal Properties of Halogen-Ethane Glassy Crystals: Effects of Orientational Disorder and the Role of Internal Molecular Degrees of Freedom. *J. Chem. Phys.* **2015**, *143*, 084510.

[12] Perez, S. C.; Zuriaga, M. J.; Serra, P.; Wolfenson, A.; Negrier, P.; Tamarit, J.Ll. Dynamic Characterization of Crystalline and Glass Phases of Deuterated 1,1,2,2 Tetrachloroethane. *J. Chem. Phys.* **2015**, *143*, 134502.

[13] Negrier, Ph.; Barrio, M.; Tamarit, J.Ll.; Mondieig, D. Polymorphism in 2-X-Adamantane Derivatives (X = Cl, Br). *J. Phys. Chem. B* **2014**, *118*, 9595–9603.

[14] Negrier, Ph.; Barrio, M.; Romanini, M.; Tamarit, J.Ll.; Mondieig, D.; Krivchikov, A.I.; Kepinski, L.; Jezowski, A.; Szewczyk, D. Polymorphism of 2-Adamantanone. *Cryst. Growth Des.* **2014**, *14*, 2626−2632.

[15] Tycko, R.; Dabbagh, G.; Fleming, R.M.; Haddon, R.C.; Makhija, A.V.; Zahurak, S.M. Molecular-Dynamics and the Phase Transition in C_{60}. *Phys. Rev. Lett.* **1991**, *67*, 1886–1889.

[16] David, W.I.F.; Ibberson, R.M.; Matthewman, J.C.; Prassides, K.; Dennis, T.J.S.; Hare, J.P.; Kroto, H.W.; Taylor, R.; Walton, D.R.M. Crystal Structure and Bonding of Ordered C_{60}. *Nature* **1991**, *353*, 147–149.

[17] Goldoni, A.; Cepek, C.; Larciprete, R.; Sangaletti, L.; Pagliara, S.; Paolucci, G.; Sancrotti, M. Core Level Photoemission Evidence of Frustrated Surface Molecules: A Germ of Disorder at the (111) Surface of C_{60} before the Order-Disorder Surface Phase Transition. *Phys. Rev. Lett.* **2002**, *88*, 196102.

[18] Macovez, R.; Goldoni, A.; Petaccia, L.; Marenne, I.; Brühwiler, P.A.; Rudolf, P. Reversible Phase Transformation and Doubly Charged Anions at the Surface of Simple Cubic RbC_{60}. *Phys. Rev. Lett.* **2008**, 101, 236403.

[19] Ramos, M.A.; Vieira, S.; Bermejo, F.J.; Dawidowski, J.; Fischer, H.E.; Schober H.; González, M.A.; Loong, C.K.; Price, D.L. Quantitative Assessment of the Effects of Orientational and Positional Disorder on Glassy Dynamics. *Phys. Rev. Lett.* **1997**, *78*, 82–85.

[20] Benkhof, S.; Kudlik, A.; Blochowicz, T.; Rössler, E. Two Glass Transitions in Ethanol: a Comparative Dielectric Relaxation Study of the Supercooled Liquid and the Plastic Crystal. *J. Phys. Condens. Matter* **1998**, *10*, 8155.

[21] Jiménez-Ruiz, M.; Gonzáles, M.A.; Bermejo, F.J.; Miller, M.A.; Birge, N.O.; Cendoya, I.; Alegría, A. Relaxational Dynamics in the Glassy, Supercooled Liquid, and Orientationally

Disordered Crystal Phases of a Polymorphic Molecular Material. *Phys. Rev. B* **1999**, *59*, 9155-9166.

[22] Götz, M.; Bauer, Th.; Lunkenheimer, P.; Loidl, A. Supercooled-Liquid and Plastic-Crystalline State in Succinonitrile-Glutaronitrile Mixtures. *J. Chem. Phys.* **2014**, *140*, 094504.

[23] Ben Hassine, B.; Negrier, Ph.; Romanini, M.; Barrio, M.; Macovez, R.; Kallel, A.; Mondieig, D.; Tamarit, J. Ll. Structure and Reorientational Dynamics of 1-F-Adamantane. *Phys. Chem. Chem. Phys.* **2016**, *18*, 10924–10930

[24] Romanini, M.; Barrio, M.; Capaccioli, S.; Macovez, R.; Ruiz-Martin, M.D.; Tamarit, J. Ll. Double Primary Relaxation in a Highly Anisotropic Orientational Glass-former with Low-dimensional Disorder. *J. Phys. Chem. C, accepted.*

[25] Gugenberger, F.; Heid, R.; Meingast, C.; Adelmann, P.; Braun, M.; Wuhl, H.; Haluska, M.; Kuzmany, H. Glass-Transition in Single Crystal C_{60} Studied by High-Resolution Dilatometry. *Phys. Rev. Lett.* **1992**, *69*, 3774–3777.

[26] Heiney, P.A.; Fischer, J.E.; McGhie, A.R.; Romanow, W.J.; Denenstein, A.M.; McCauley, J.P.; Smith, A.B.; Cox, D.E. Orientational Ordering Transition in Solid C_{60}. *Phys. Rev. Lett.* **1991**, *66*, 2911–2914.

[27] Mehring, M.; Their, K.F.; Rachdi, F.; de Swiet, T. Localized and Delocalized Electronic States in A(1)C(60) (A=Rb, Cs). *Carbon* **2000**, *38*, 1625–1633.

[28] Neretin, I.S.; Slovokhotov, Y.L. Chemical Crystallography of Fullerenes. *Russ. Chem. Rev.* **2004**, *73*, 455–486.

[29] Pekker, S.; Kováts, É.; Oszlányi, G.; Bényei, G.; Klupp, G.; Bortel, G.; Jalsovszky, I.; Jakab, E.; Borondics, F.; Kamarás, K.; Bokor, M.; Kriza, G.; Tompa, K.; Faigel, G. Rotor–Stator Molecular Crystals of Fullerenes with Cubane. *Nat. Mater.* **2005**, *4*, 764–767.

[30] Collins, C.; Foulkes, J.; Bond, A.D.; Klinowski, J. Crystalline C_{60}·$2CHBr_3$ Solvate: a Solid-State Study. *Phys. Chem. Chem. Phys.* **1999**, *1*, 5323–5326.

[31] Mitsari, E.; Romanini, M.; Zachariah, M.; Macovez, R. Solid State Physicochemical Properties and Applications of Organic and Metallo-Organic Fullerene Derivatives. *Curr. Org. Chem.* **2016**, *20*, 645–661.

[32] Michaud, F.; Barrio, M.; Lopez, D.O.; Tamarit, J.Ll.; Agafonov, V.; Toscani, S.; Szwarc, H.; Céolin, R. Solid-State Studies on a C_{60} Solvate Grown from 1,1,2-Trichloroethane. *Chem. Mater.* **2000**, *12*, 3595–3602.

[33] Barrio, M.; Lopez, D.O.; Tamarit, J.Ll.; Espeau, P.; Céolin R.; Allouchi, H. Solid-State Studies of C_{60} Solvates Formed in the C_{60}-$BrCCl_3$ System. *Chem. Mater.* **2003**, *15*, 288–291.

[34] Toscani, S.; Allouchi, H.; Tamarit, J.Ll.; Lopez, D.O.; Barrio, M.; Agafonov, V.; Rassat, A.; Szwarc, H.; Céolin, R. Decagonal C_{60} Crystals Grown From n-Hexane Solutions: Solid-State and Aging Studies. *Chem. Phys. Lett.* **2000**, *330*, 491–496.

[35] Faigel, G.; Bortel, G.; Oszlányi, G.; Pekker, S.; Tegze, M.; Stephens, P.W.; Liu, D. Low-Temperature Phase Transition in C_{60}-n-Pentane. *Phys. Rev. B* **1994**, *49*, 9186–9189.

[36] Collins, C.; Duer, M.; Klinowski, J. Molecular Dynamics in Crystalline C_{60} · $2CHBr_3$. *Chem Phys. Lett.* **2000**, *321*, 287–291.

[37] Rozen, J.; Masin, F.; Ceolin, R.; Szwarc, H. Dynamical Model for the C_5H_5 Cycles in the $C_{60} \cdot 2Fe(C_5H_5)_2$ Solvate. *Phys. Rev. B* **2004**, *70*, 144206.

[38] Masin, F.: Gall, D.; Gusman, G. ^{13}C NMR Spectroscopy of Chloroform-Solvated-C_{60}. *Solid State Commun.* **1994**, *91*, 849–852.

[39] Masin, F.; Grell, A.-S.; Messari, I.; Gusman, G. Benzene-Solvated C_{60}: ^{1}H Nuclear Spin-Lattice Magnetic Relaxation. *Solid State Commun*. **1998**, *106*, 59–62.

[40] Grell, A.-S.; Masin, F.; Céolin, R.; Gardette, M. F.; Szwarc, H. Molecular Dynamics of $C_{60}.2S_8$: a ^{13}C NMR Study. *Phys. Rev. B* **2000**, *62*, 3722–3727.

[41] Bousige, C.; Rols, S.; Cambedouzou, J.; Verberck, B.; Pekker, S.; Kováts, É.; Durkó, G.; Jalsovsky, I.; Pellegrini, É.; Launois, P. Lattice Dynamics of a Rotor-Stator Molecular Crystal: Fullerene-Cubane $C_{60} \cdot C_8H_8$. *Phys. Rev. B* **2010**, *82*, 195413.

[42] Ngai, K.L.; Capaccioli, S.; Ancherbak, S.; Shinyashiki, N. Resolving the Ambiguity of the Dynamics of Water and Clarifying its Role in Hydrated Proteins. *Philos. Mag.* **2011**, *91*, 1809–1835.

[43] Capaccioli, S.; Ngai, K.L. Resolving the Controversy on the Glass Transition Temperature of Water? *J. Chem. Phys.* **2011**, *135*, 104504.

[44] Einfeldt, J.; Kwasniewski, A. Characterization of Different Types of Cellulose by Dielectric Spectroscopy. *Cellulose* **2002**, *9*, 225–238.

[45] Bujak, M.; Podsiadło, M.; Katrusiak, A. Energetics of Conformational Conversion between 1,1,2-Trichloroethane Polymorphs. *Chem. Commun.* **2008**, *37*, 4439–4441.

[46] Hebard, A.F.; Haddon, R.C.; Fleming, R.M.; Kortan, A.R. Deposition and Characterization of Fullerene Films. *Appl. Phys. Lett.* **1991**, *59*, 2109–2111.

[47] Pederson, M.R.; Quong, A.A. Polarizabilities, Charge States, and Vibrational-Modes of Isolated Fullerene Molecules. *Phys. Rev. B* **1992**, *46*, 13584–13591.

[48] Macovez, R.; Hunt, M.R.C.; Goldoni, A.; Pedio, M.; Rudolf, P. Surface Hubbard U of Alkali Fullerides. *J. Electron. Spectrosc.* **2011**, *183*, 94–100.

[49] Oszlanyi, G.; Bortel G.; Faigel, G.; Pekker, S.; Tegze, M.; Cernik, R.J. Mechanically Induced Chemical Decomposition of C_{60}-*n*-Pentane Clathrate at Room-Temperature. *Phys. Rev. B* **1993**, *48*, 7682–7684.

[50] Michaud, F.; Barrio, M.; Toscani, S.; Lopez, D.O.; Tamarit, J.Ll.; Agafonov, V.; Szwarc, H.; Céolin, R. Solid-State Studies on Single and Decagonal Crystals of C_{60} Grown from 1,2-Dichloroethane. *Phys. Rev. B* **1998**, *57*, 10351–10358.

[51] Olmstead, M.M.; Jiang, F.; Balch, A.L. $2C_{60}{\cdot}3CS_2$: Orientational Ordering Accompanies the Reversible Phase Transition at 168 K. *Chem. Commun.* **2000**, *6*, 483–484.

[52] Balch, A.L.; Lee, J.W.; Noil, B.C.; Olmstead, M.M. Disorder in a Crystalline Form of Buckminsterfullerene: $C_{60}{\cdot}4C_6H_6$. *J. Chem. Soc., Chem. Commun.* **1993**, *1*, 56–58.

[53] Korobov, M.V.; Mirakian, A.L.; Avramenko, N.V.; Valeev, E.F.; Neretin, I.S.; Slovokhotov, Y.L.; Smith, A.L.; Olofsson, G.; Ruoff, R.S. C_{60}·Bromobenzene Solvate: Crystallographic and Thermodynamical Studies and their Relationship to C_{60} Solubility in Bromobenzene. *J. Phys. Chem. B* **1998**, *102*, 3712–3717.

[54] Geiser, U.; Kumar, S.K.; Savall, B.M.; Harried, S.S.; Carlson, K.D.; Mobley, P.R.; Wang, H.H.; Williams, J.M.; Botto, R.E. Discrete Layers of Ordered C_{60} Molecules in the Co-Crystal $C_{60}{\cdot}CH_2I_2{\cdot}C_6H_6$: Synthesis, Crystal Structure, and ^{13}C NMR Properties. *Chem. Mater.* **1992**, *4*, 1077–1082.

[55] Havrilliak, S.; Negami, S. A Complex Plane Analysis of α-Dispersions in Some Polymer Systems. *J. Polym. Sci. Part C* **1966**, *14*, 99–117.

[56] Havrilliak, S.; Negami, S. A Complex Plane Representation of Dielectric and Mechanical Relaxation Processes in Some Polymers. *Polymer* **1967**, *8*, 161–210.

[57] Böttcher, C.J.F.; Bordewijk, P. *Theory of Electric Polarization. Volume II: Dielectrics in Time-Dependent Fields*. Amsterdam: Elsevier Science, 1978.

[58] Saito, S.; Oshiyama, A. Cohesive Mechanism and Energy Bands of Solid C_{60}. *Phys. Rev. Lett.* **1991**, *66*, 2637-2640.

[59] Buin, A.; Wang, H.; Consta, S.; Huang, Y. A Study of Conformational Equilibrium of 1,1,2-Trichloroethane in FAU-Type Zeolites. *Micropor. Mesopor. Mat.* **2014**, *183*, 207–217.

[60] Iribarren, J.I.; Casanovas, J.; Zanuy, D.; Aleman, C. Influence of the Solvation Model and the Solvent on the Gauche-Trans Equilibrium of 1,1,2-Trichloroethane. *Chem. Phys.* **2004**, *302*, 77–83.

[61] Kuratani, K.; Mizushima, S. Infrared Absorption Investigation on the Rotational Isomerism of 1,1,2-Trichloroethane. *J. Chem. Phys.* **1954**, *22*, 1403–1405.

[62] Christian, S.D.; Grundnes, J.; Klaeboe, P.; Nielsen, C.J.; Woldbaek, T. Vibrational and high-Pressure Conformational Studies of 1,1,2-Trichloroethane. *J. Mol. Struct.* **1976**, *34*, 33–45.

[63] Christian, S.D.; Grundnes, J.; Klaboe, P. Pressure Effects on Conformational Equilibria - Difference in Volume Between Conformers of 1,1,2-Trichloroethane. *J. Chem. Phys.* **1976**, *65*, 496–498.

[64] Nomura, H.; Koda, S.; Hamada, K. Study of the Conformational Equilibria Between Rotational Isomers Using Ultrasonic Relaxation and Raman Spectroscopy Part2. Di- and Trihalogenoalkanes. *J. Chem. Soc., Faraday Trans. 1* **1988**, *84*, 1267–1275.

[65] Allen, G.; Brier, P.N.; Lane, G. Spectroscopic Study of Internal Rotation in Chloroethanes. *Trans. Faraday Soc.* **1967**, *63*, 824–832.

[66] Macovez, R.; Lopez, N.; Mariano, M.; Maymò, M.; Martorell, J. Molecular Conformation in Organic Films from Quantum Chemistry Ab Initio Calculations and Second Harmonic Spectroscopy. *J. Phys. Chem. C* **2012**, *116*, 26784−26790.

[67] Semkin, V.N.; Spitsina, N.G.; Graja, A. FT IR Transmission Spectral Study of Some Single-Crystals of C_{60} Clathrates. *Chem. Phys. Lett.* **1995**, *233*, 291–297.

[68] Swietlik, R.; Byszewski, P.; Kowalska, E. Interactions of C_{60} with Organic Molecules in Solvate Crystals Studied by Infrared Spectroscopy. *Chem. Phys. Lett.* **1996**, *254*, 73–78.

[69] Macovez, R.; Zachariah, M.; Romanini, M.; Zygouri, P.; Gournis, D.; Tamarit, J.Ll. Hopping Conductivity and Polarization Effects in a Fullerene Derivative Salt. *J. Phys. Chem. C* **2014**, *118*, 12170–12175.

[70] Kremer, F.; Schönhals, A. *Broad Band Dielectric Spectroscopy*. Berlin: Springer; 2003, pp. 59-129.

[71] Kirkwood, J.G. The Dielectric Polarization of Polar Liquids. *J. Chem. Phys.* **1939**, *7*, 911–919.

[72] Tripathi, P.; Mitsari, E.; Romanini, M.; Serra, P.; Tamarit, J. Ll.; Zuriaga, M.; Macovez, R. Orientational Relaxations in Solid (1,1,2,2)-Tetrachloroethane. *J. Chem. Phys.* **2016**, *144*, in press.